

**Environmental effects on electron spin relaxation in N@C<sub>60</sub>**John J. L. Morton,<sup>1,2,\*</sup> Alexei M. Tyryshkin,<sup>3</sup> Arzhang Ardavan,<sup>1,2</sup> Kyriakos Porfyrikis,<sup>1</sup> S. A. Lyon,<sup>3</sup> and G. Andrew D. Briggs<sup>1</sup><sup>1</sup>*Department of Materials, Oxford University, Oxford OX1 3PH, United Kingdom*<sup>2</sup>*Clarendon Laboratory, Department of Physics, Oxford University, Oxford OX1 3PU, United Kingdom*<sup>3</sup>*Department of Electrical Engineering, Princeton University, Princeton, New Jersey 08544, USA*

(Received 17 April 2007; published 16 August 2007)

We examine environmental effects of surrounding nuclear spins on the electron spin relaxation of the N@C<sub>60</sub> molecule (which consists of a nitrogen atom at the center of a fullerene cage). Using dilute solutions of N@C<sub>60</sub> in regular and deuterated toluene, we observe and model the effect of translational diffusion of nuclear spins of the solvent molecules on the N@C<sub>60</sub> electron spin relaxation times. We also study spin relaxation in frozen solutions of N@C<sub>60</sub> in CS<sub>2</sub>, to which small quantities of a glassing agent, S<sub>2</sub>Cl<sub>2</sub>, are added. At low temperatures, spin relaxation is caused by spectral diffusion of surrounding nuclear <sup>35,37</sup>Cl spins in the S<sub>2</sub>Cl<sub>2</sub>, but, nevertheless, at 20 K, T<sub>2</sub> as long as 0.23 ms is observed.

DOI: 10.1103/PhysRevB.76.085418

PACS number(s): 76.30.-v, 81.05.Tp

**I. INTRODUCTION**

The N@C<sub>60</sub> molecule is well known for its remarkably well-shielded electron spin,<sup>1</sup> prompting several proposals for fullerene-based quantum information processing (QIP).<sup>2,3</sup> Indeed, extraordinarily long electron spin relaxation times, satisfying the strict requirements for QIP,<sup>2</sup> have been reported for N@C<sub>60</sub> in liquid solutions<sup>4,5</sup> and in solid matrices,<sup>2</sup> thus demonstrating the capacity of the fullerene cage for protecting the enclosed spin from fluctuating perturbations in various host environments. This property opens the possibility of using almost any host material when “designing” N@C<sub>60</sub>-based QIP processors. For example, proposed architectures include N@C<sub>60</sub> arrays positioned at interfaces (e.g., arranged on solid templates) where they would be expected to be exposed to a broad spectrum of environmental perturbations.

Two important spin relaxation mechanisms have recently been identified for N@C<sub>60</sub> in liquid solutions,<sup>1,5</sup> both involving the internal motion of the fullerene cage (e.g., vibrational or rotational motion). These two mechanisms explain a large body of the experimental data. An Orbach mechanism via a vibrational mode of the C<sub>60</sub> cage was shown to determine the spin relaxation of N@C<sub>60</sub> in a CS<sub>2</sub> solvent environment over a broad range of temperatures.<sup>5</sup> The Orbach relaxation mechanism involves an interaction with two phonons whose energy difference matches the energy splitting of the relevant spin states and which are resonant with a transition to an excited electronic state (i.e., a vibrational or an orbital state which lies outside of the space considered by the spin Hamiltonian). Nevertheless, this Orbach mechanism remains weak, resulting in very long relaxation times (T<sub>1</sub>=0.5 ms and T<sub>2</sub>=0.24 ms at 160 K, just above the melting point of CS<sub>2</sub>). Even longer relaxation times might be expected at lower temperatures; however, the CS<sub>2</sub> solvent is not suitable for frozen solution studies since it freezes as a polycrystal with consequent grain boundary segregation of the dissolved fullerene molecules.

A second relaxation mechanism was found for asymmetric N@C<sub>70</sub> fullerenes, which possess a permanent zero field

splitting (ZFS).<sup>5</sup> A random rotational reorientation of this ZFS contributes significantly to N@C<sub>70</sub> spin relaxation at temperatures lower than 260 K, a temperature range in which rotational mobility is insufficient to achieve efficient motional averaging of the nonzero ZFS.

Relaxation of N@C<sub>60</sub> (and N@C<sub>70</sub>) in solid matrices has not been comprehensively studied yet. Very long T<sub>1</sub> ~ 1 s have been reported in low-purity N@C<sub>60</sub>/C<sub>60</sub> powders at 4 K, while considerably shorter T<sub>2</sub>=20 μs were found.<sup>2</sup> The mechanism behind such an unexpectedly short T<sub>2</sub> remains unexplained.

In this paper, we extend the studies of electron spin relaxation of N@C<sub>60</sub> and examine the role of nuclear spins in the solvent environment, both in liquids and in frozen solutions. The CS<sub>2</sub> solvent used in our previous studies had no naturally abundant nuclear spins (i.e., only 1.1% of <sup>13</sup>C with nuclear spin I=1/2 and 0.76% of <sup>33</sup>S with I=3/2). In this work, we use a toluene solvent and a CS<sub>2</sub>/S<sub>2</sub>Cl<sub>2</sub> mixture: both contain substantial numbers of magnetic nuclei. We show how the presence of a high concentration of nuclear spins from solvent molecules can significantly shorten the relaxation time of N@C<sub>60</sub>. Depending on the temperature regime, i.e., liquid or frozen solutions, the translational<sup>6</sup> or spin<sup>7-10</sup> diffusion of nuclear spins surrounding the N@C<sub>60</sub> molecule contributes to electron spin relaxation.

**II. MATERIALS AND METHODS**

The aggregation (or clustering) of C<sub>60</sub> in certain solvents and concentrations has been widely reported.<sup>11-17</sup> Furthermore, the solubilities of C<sub>60</sub> in toluene and in CS<sub>2</sub> show a strong temperature dependence peaking at 280 K and falling rapidly upon further cooling.<sup>18</sup> The result is that the convenient picture of isolated fullerenes in solution is rather naive; instead, the behavior is a complex nonmonotonic function of temperature, fullerene concentration, choice of solvent, and even time from initial dissolution. For example, in CS<sub>2</sub> at room temperature, the onset of aggregation has been measured to be at a concentration of around 0.06 mg/ml.<sup>11</sup> At concentrations above 0.36 mg/ml, the clusters themselves

further agglomerate to form “flowerlike” structures with an open hole in the center. In toluene, clusters ranging from 3 to 55 fullerenes have been observed over a dilute range of concentrations (0.18–0.78 mg/ml).<sup>17</sup> This clustering can have important consequences on electron spin relaxation rates, resulting in a distribution of the relaxation times depending on the location of  $N@C_{60}$  within the cluster. An additional complication can arise in samples of higher  $N@C_{60}/C_{60}$  purity—if the large  $C_{60}$  cluster contains two  $N@C_{60}$  molecules, their relaxation will be strongly affected by the dipole-dipole interaction between the two  $N@C_{60}$  electron spins. For example, in a sample of 3%  $N@C_{60}/C_{60}$  purity, we have observed a decrease in  $T_2$  with increasing fullerene concentration above about 0.1 mg/ml.

To eliminate uncertainties associated with  $C_{60}$  cluster formation, dilute solutions with concentrations of less than 0.06 mg/ml were used in this study. High-purity ( $\approx 80\%$ ) endohedral  $N@C_{60}$  was used to prepare samples in toluene, enabling the use of dilute solutions (2  $\mu\text{g}/\text{ml}$ ) of well-isolated fullerenes, which nevertheless provide a sufficient signal for pulsed EPR experiments. Solutions were degassed by freeze pumping in three cycles to remove paramagnetic  $O_2$ . We observe that while samples of  $N@C_{60}$  in  $CS_2$  are stable, the EPR signal from the sample in degassed toluene decayed when exposed to light. The precise nature of this decay is unknown and possibly occurs via the photoexcited triplet state of the  $C_{60}$  cage, leading to the escape of the nitrogen from the cage. Other experimental parameters, including a brief description of the  $N@C_{60}$  spin system are provided elsewhere.<sup>5</sup>  $T_2$  and  $T_1$  measurements were performed using Hahn echo and inversion recovery sequences, respectively.<sup>19</sup>

Given the strong reactivity of  $S_2Cl_2$ , there was some concern that it might attack the fullerenes in the solution—this dictated the sample preparation procedure adopted. 50  $\mu\text{l}$  samples of  $N@C_{60}$  (4% purity) in  $CS_2$  and pure  $S_2Cl_2$  were degassed in two separate arms of a  $\lambda$ -shaped quartz vessel. The solvents were then mixed and quickly frozen; the resulting mixture contained approximately 25%  $S_2Cl_2$  by volume (corresponding to 20 mol %).

### III. SPIN RELAXATION OF $N@C_{60}$ IN TOLUENE SOLUTION

When  $N@C_{60}$  is dissolved in a solution containing nuclear spins (such as the hydrogen atoms of toluene), additional relaxation pathways may be introduced. These arise from fluctuating fields caused by the motion of solvent molecules around the fullerene cage. The use of both regular (hydrogenated) and deuterated toluene as solvents can provide further insights into the effect of local nuclear spins. Figures 1 and 2 show  $T_1$  and  $T_2$  measured for high-purity  $N@C_{60}$  in toluene solution, as a function of temperature.

The temperature dependence of  $T_1$  in toluene is suggestive of an Orbach relaxation mechanism, similar to that reported for  $N@C_{60}$  in  $CS_2$ .<sup>5</sup> However, the slopes of the temperature dependence are markedly different in the two solvents. In  $CS_2$ , the energy splitting derived from the slope matched well the first excited  $H_g(1)$  vibrational mode of  $C_{60}$

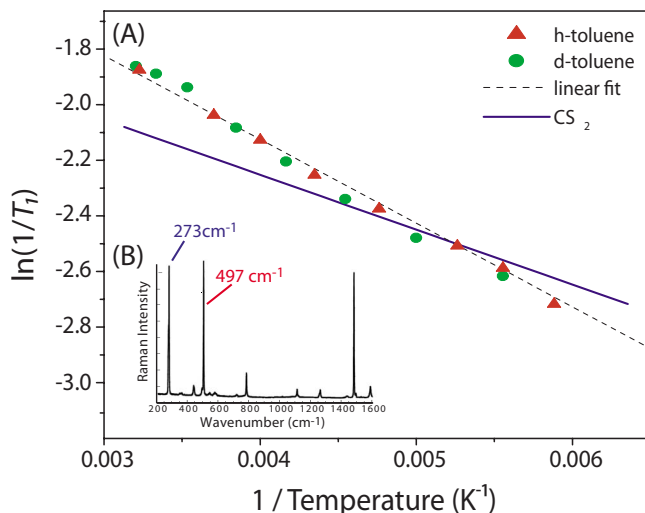


FIG. 1. (Color online) (A) Spin relaxation time  $T_1$  for  $N@C_{60}$  in toluene as a function of temperature, plotted as  $\ln(1/T_1)$  against  $(1/T)$ , where  $T_1$  is given in microseconds.  $T_1$  values are indistinguishable for regular toluene (triangles) and deuterated toluene (circles). The linear fit (dashed line) is consistent with an Orbach relaxation mechanism, and the slope to the fit gives an energy splitting  $\Delta=60(2)$  meV of the excited state involved in the relaxation process. A similar linear dependence has been reported for  $N@C_{60}$  in  $CS_2$  (Ref. 5), but the linear fit (solid line) gave a different  $\Delta=33$  meV. (B) Two major absorption peaks in the Raman spectrum of  $C_{60}$  lie at 273 and 497  $\text{cm}^{-1}$  (33 and 62 meV, respectively).

at 33 meV, and in toluene, the slope corresponds to an energy splitting of 60(2) meV, which coincides with the second major line seen in the Raman spectra (62 meV), corresponding to the  $A_g(1)$  mode [Fig. 1(b)]. Solvent effects have been reported extensively in the Raman spectroscopy of  $C_{60}$ ,<sup>20</sup> and

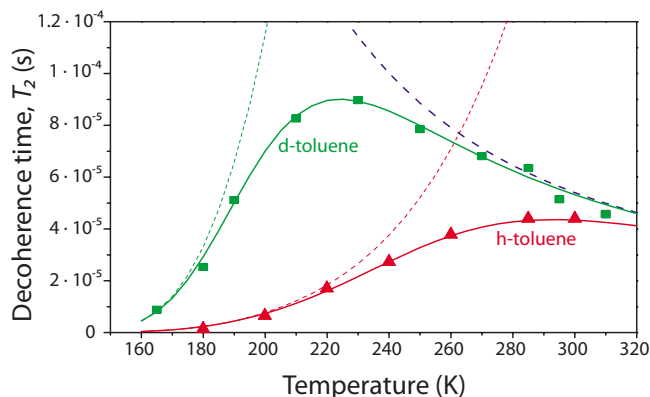


FIG. 2. (Color online) Spin decoherence time  $T_2$  of  $N@C_{60}$  in toluene, measured using the central  $M_I=0$  line, with regular toluene (red triangles) and deuterated toluene (green squares). The solid curves are generated using the model that involves two relaxation mechanisms, and the broken curves show individual contributions of the two mechanisms. The (blue) dashed curve is the “intrinsic” decoherence time due to the Orbach relaxation process;  $T_2=2/3T_1$  is assumed based on the study of  $N@C_{60}$  in  $CS_2$  (Ref. 5). The (red and green) dotted curves show the relaxation effect due to translational diffusion of proton and deuterium nuclei of toluene molecules.

it is concluded that the nature of the solvent-fullerene interaction can distort the icosahedral symmetry, leading to splittings of the  $H_g$  Raman transitions.<sup>21</sup> Consistently, the results here could also be attributed to interactions between the cage and the solvent (e.g., a  $\pi$ -stacking arrangement in the case of the aromatic toluene molecule); the transitions involving the  $H_g(1)$  mode may be suppressed, and electron spin relaxation of the endohedral nitrogen takes places more effectively via the higher-energy  $A_g(1)$  squeezing mode.

The  $T_2$  relaxation data in Fig. 2 reveal a nonmonotonic temperature dependence in contrast to that observed for N@C<sub>60</sub> in CS<sub>2</sub>.<sup>5</sup> In CS<sub>2</sub>, a simple ratio of  $T_2=2/3T_1$  was found over the broad temperature range, indicating that both  $T_1$  and  $T_2$  are determined by the same Orbach relaxation mechanism. In toluene,  $T_2$  diverges noticeably from the  $T_1$  dependence, indicating that an additional relaxation mechanism must be involved, which suppresses  $T_2$  at low temperatures. In the following discussion, we argue that this additional relaxation mechanism is due to nuclear spins (protons) of the toluene solvent.

In liquid solutions, solvent molecules can diffuse around N@C<sub>60</sub>. Therefore, the distance between the electron spin of N@C<sub>60</sub> and the nuclear spins of toluene molecules changes in time. This results in fluctuating hyperfine (contact and dipolar) fields seen by the electron spin, which can drive its relaxation. In the hard-sphere approximation, the spin-spin separation varies between a value called the *distance of closest approach* ( $d$ ) and infinity. The translation diffusion time  $\tau_D$  becomes the important correlation time,<sup>6</sup>

$$\tau_D = \frac{2d^2}{D(T)}, \quad (1)$$

where  $D(T)=D_{C_{60}}(T)+D_{\text{tol}}(T)$  is the sum of the temperature-dependent diffusion coefficients of the fullerene and toluene molecules. According to common models for diffusion-induced spin relaxation,<sup>22-24</sup> the resulting  $T_1$  and  $T_2$  are<sup>6</sup>

$$(T_1)^{-1} = 2\kappa \frac{c(T)}{d \cdot D(T)} 10J(\omega_e), \quad (2)$$

$$(T_2)^{-1} = \kappa \frac{c(T)}{d \cdot D(T)} [4J(0) + 10J(\omega_e) + 6J(\omega_n)]. \quad (3)$$

$\omega_e$  and  $\omega_n$  are the electron and nuclear Zeeman frequencies, respectively. The constant prefactor  $\kappa$  is given by

$$\kappa = \frac{16\pi}{405} \gamma_e^2 \gamma_n^2 \hbar^2 I(I+1). \quad (4)$$

$\gamma_e$  and  $\gamma_n$  are the electron and nuclear gyromagnetic ratios,  $c(T)$  is the temperature-dependent concentration of hydrogen (or deuterium) spins, and the spectral density function  $J(\omega)$  is given by

$$J(\omega) = \frac{1 + 5z/8 + z^2/8}{1 + z + z^2 + z^3/6 + 4z^4/81 + z^5/81 + z^6/648}, \quad (5)$$

with  $z = \sqrt{2\omega\tau_D}$ .

The only unknown quantities in the above expressions are nuclear spin concentration  $c(T)$ , distance of closest approach

$d$ , and the diffusion coefficient  $D(T)$ . The temperature dependence of <sup>1</sup>H concentration in toluene is given in Ref. 29 as

$$c(T) = (4.089 \times 10^{21})(0.266 55^{-[1+(1-7/591.8)^{0.2878}]}) \quad (6)$$

and varies between about  $(4.5-5) \times 10^{22} \text{ cm}^{-3}$  over the temperature range 150–300 K. Evidently, the variation in this parameter is not great and therefore could not explain the temperature dependence of  $T_2$ . It must be  $D(T)$  and its strong temperature dependence that dominates the effect on  $T_2$ .

The self-diffusion coefficient  $D(T)$  of toluene has been studied as a function of temperature.<sup>25</sup> In the temperature range 135–330 K, the data are fitted well to

$$D_{\text{tol}}(T) = 6.1 \times 10^{-4} \exp\left(-\frac{1000}{T}\right) \exp\left[-\left(\frac{190}{T}\right)^6\right] \text{ cm}^2/\text{s}. \quad (7)$$

The diffusion coefficient for C<sub>60</sub> can be roughly estimated by the Stokes-Einstein equation

$$D_{C_{60}}(T) = \frac{k_B T}{6\pi a \eta(T)}, \quad (8)$$

where  $a=0.35 \text{ nm}$  is the radius of the N@C<sub>60</sub> molecule and  $\eta(T)$  is the solvent viscosity which can also be temperature dependent. However, reports on toluene viscosity only go down to 225 K,<sup>26</sup> below which one would expect substantial changes in behavior. As a result, both  $D_{C_{60}}(T)$  and  $d$  were left as fitting parameters.

To fit the experimental data in Fig. 2, we assume two relaxation processes: the translational diffusion mechanism described above and the Orbach relaxation mechanism, which, if alone, would produce  $T_2=2/3T_1$ , as was found for N@C<sub>60</sub> in CS<sub>2</sub> solution.<sup>5</sup> The individual contribution of each of the two relaxation mechanisms and their overall effect are shown in Fig. 2. The best fit was achieved using a diffusion coefficient whose temperature dependence is shown in Fig. 3, and  $d=0.35 \text{ nm}$  (though it was possible to obtain reasonable fits for  $d$  up to about 0.45 nm). The radius of the C<sub>60</sub> molecule is 0.35 nm, so these values for the distance of closest approach are reasonable. The best-fit diffusion coefficient of C<sub>60</sub> converges with that predicted by the Stokes-Einstein equation [Eq. (8)] for temperatures below 250 K; however, it deviates by as much as a factor of 10 at higher temperatures (310 K).

Finally, evaluating Eq. (2) with the parameters extracted from the study of  $T_2$ , we see that the  $T_1$  values for  $h$ -toluene and  $d$ -toluene are expected to be equal, as the translational diffusion  $T_1$  rates are much slower than the intrinsic (Orbach) decay mechanism (see Fig. 4).

#### IV. SPIN RELAXATION OF N@C<sub>60</sub> IN A FROZEN SOLUTION

A glass-forming solvent is essential for frozen solution studies of N@C<sub>60</sub> in order to ensure homogeneity of the frozen solution and to avoid clustering of N@C<sub>60</sub>. The ideal solvent would also contain a minimal concentration of nuclear spins since it is known that nuclear spins of the sol-

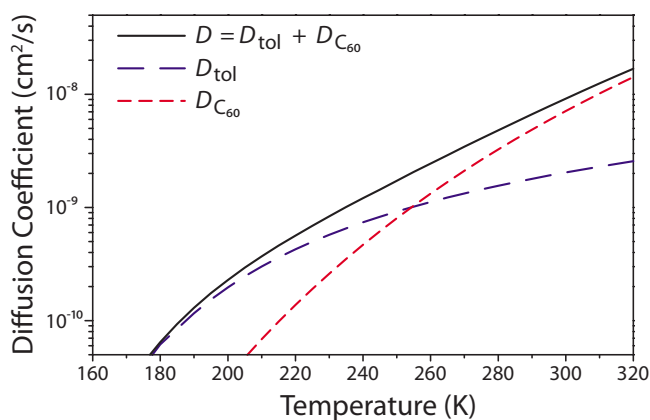


FIG. 3. (Color online) Temperature dependence for the (dashed blue curve) self-diffusion coefficient of toluene,  $D_{\text{tol}}$ , based on experimental results (Ref. 25); (dashed red curve) the predicted diffusion coefficient of  $C_{60}$  in toluene,  $D_{C_{60}}$ , which produces the best fits to the data in Fig. 2; (solid black curve) the overall diffusion coefficient,  $D = D_{\text{tol}} + D_{C_{60}}$ .

vent molecules can provide a significant mechanism for electron spin decoherence, e.g., via the process known as *spectral diffusion* caused by flip-flops of the local nuclear spins.<sup>7-9</sup> While such an ideal solvent has not come to our attention, it is possible to add relatively small quantities of sulphur chloride ( $S_2Cl_2$ ) to  $CS_2$  to act as a glassing agent.<sup>27</sup> The addition of 15 mol %  $S_2Cl_2$  in  $CS_2$  is sufficient to permit vitrification of small samples.  $CS_2$  has no major isotopes with nonzero nuclear spins: however,  $S_2Cl_2$  has chlorine whose major isotopes both have nuclear spin  $I = 3/2$  and gyromagnetic ratios of about 4 MHz/T. Therefore, while this mixture is not an optimal solution, it was hoped that the reduced nuclear spin concentration in the mixture solution would permit relatively long decoherence times, not limited by the nuclear spectral diffusion.

The measured  $T_1$  and  $T_2$  are shown in Figs. 5 and 6 in the temperature range 20–165 K (below the melting point of the

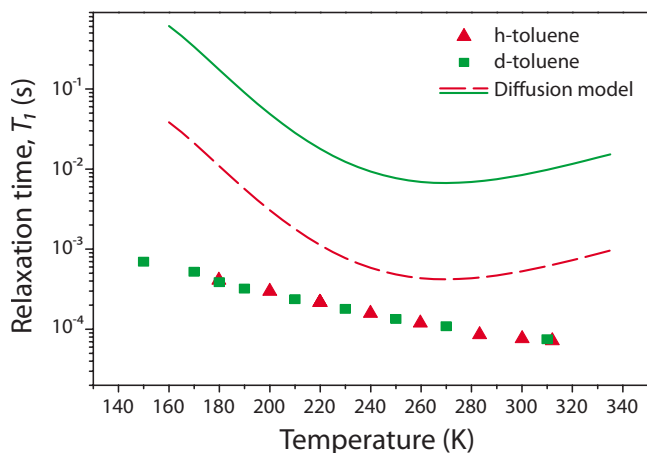


FIG. 4. (Color online) Experimental  $T_1$  values for  $N@C_{60}$  in regular (red triangles) and deuterated (green squares) toluene. Curves show theoretical  $T_1$  predicted from the model of relaxation by translational diffusion of nuclear spins in the solvent molecules [Eq. (2)].

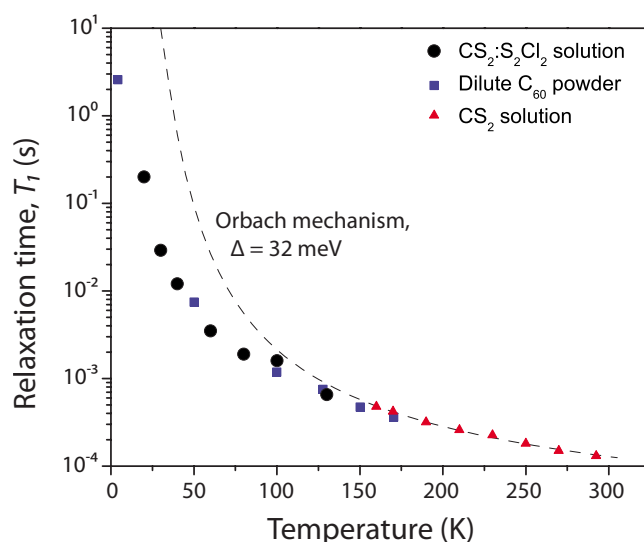


FIG. 5. (Color online) Temperature dependence of  $T_1$  for  $N@C_{60}$  in a frozen solution of  $CS_2:S_2Cl_2$  (volume 3:1), measured on the central ( $M_I = 0$ ) hyperfine line. Data for  $N@C_{60}$  diluted in  $C_{60}$  powder and in  $CS_2$  solution are shown for comparison. Dashed line is an extrapolation of the  $T_1$  data measured for  $N@C_{60}$  in  $CS_2$  assuming the Orbach relaxation mechanism in the entire temperature range.

mixture).  $T_1$ , which was measured on the central  $M_I = 0$  hyperfine line, has a monotonic temperature dependence and follows closely that seen in a dilute powder of  $N@C_{60}/C_{60}$ . It seems that the residual concentration of nuclear spins in the  $S_2Cl_2/CS_2$  mixture has no effect on  $T_1$  in the temperature range studied. However, both solid samples show  $T_1$  values which are less than that expected by extrapolating the Or-

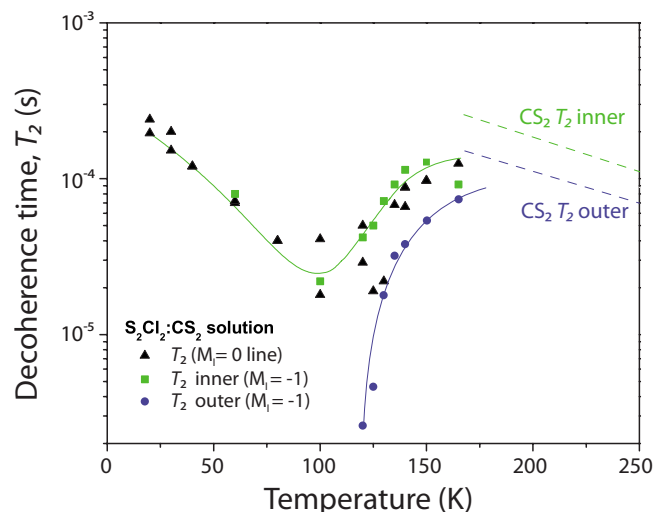


FIG. 6. (Color online) Temperature dependence of  $T_2$  for  $N@C_{60}$  in a frozen solution of  $CS_2:S_2Cl_2$  (volume 3:1), measured on the central ( $M_I = 0$ ) and high-field ( $M_I = -1$ ) hyperfine lines of the  $N@C_{60}$  EPR spectrum. For  $M_I = -1$ , two  $T_2$  values,  $T_{2o}$  and  $T_{2i}$ , are extracted for outer ( $M_S = \pm 3/2 : \pm 1/2$ ) and inner ( $M_S = +1/2 : -1/2$ ) transitions within the  $S = 3/2$  multiplet, using their different ESEEM frequencies (Ref. 5). The curves are visual guides.

bach mechanism suggested for N@C<sub>60</sub> in CS<sub>2</sub> solution. Apparently, other (yet unidentified) relaxation mechanisms contribute significantly in both solid matrices at low temperatures, resulting in  $T_1$  shorter than what would be expected from the Orbach mechanism alone. Relaxation experiments at different microwave frequencies will be required to shed light on these unidentified mechanisms.

On the other hand,  $T_2$ , when measured on the  $M_I=0$  line, shows a minimum at around 100 K, coinciding with the approximate glass transition temperature  $T_g$  of the solvent mixture.<sup>27</sup> For measurements on the  $M_I=-1$  high-field hyperfine line, two different  $T_2$  values corresponding to the outer ( $M_S=\pm 3/2:\pm 1/2$ ) and inner ( $M_S=+1/2:-1/2$ ) transitions can be separated using the electron spin echo envelope modulation (ESEEM) method described elsewhere.<sup>5</sup>  $T_{2,o}$  (outer) falls dramatically upon cooling toward  $T_g$ .  $T_{2,i}$  (inner) reaches a minimum at  $T_g$ , but then rises as the temperature is lowered further. We can now see that the  $T_2$  measured on the central line is indeed a weighted average of the two separate  $T_2$  values (inner and outer) for temperatures above  $T_g$ . Below  $T_g$ , the outer coherences decay sufficiently quickly ( $T_{2,o} < 1 \mu\text{s}$ ) to become unobservable in the spin echo experiment. Indeed, only  $T_{2,i}$  can be measured below  $T_g$ . Recognizing the fact that  $T_{2,i}$  measured for  $M_I=0$  and  $-1$  are almost identical (within the error of the experiment) in a broad temperature range below 120 K, we can conclude that a hyperfine interaction with <sup>14</sup>N nucleus has no visible effect on  $T_2$  in N@C<sub>60</sub> at low temperatures.

The fact that  $T_{2,o}$  is much shorter than  $T_{2,i}$  at low temperatures can be explained by the effect of a nonzero ZFS. The glassy solvent matrix around the fullerene imposes a distortion of the N@C<sub>60</sub> cage, inducing a ZFS strain to the nitrogen atom. At temperatures approaching  $T_g$  and below, the rotational mobility of fullerenes slows down. Therefore, a complete motional averaging of the nonzero ZFS is not achieved. In this case, the ZFS strain creates an inhomogeneous broadening of the EPR transitions, and the outer transitions within the  $S=3/2$  multiplet are broadened more significantly, i.e., via the first-order ZFS, in contrast to the inner transition, which is broadened only via the second-order ZFS. Provided that the ZFS broadening is small compared to the excitation bandwidth of the microwave pulses, and thus the second pulse in the spin echo experiment refocuses all transitions within the  $S=3/2$  multiplet, such a ZFS broadening would not be refocused for the outer coherences and would appear instead as an additional dephasing mechanism, leading to a fast decay of the outer transitions. On the other hand, the inner transition is fully refocused, and its decoherence time,  $T_{2,i}$ , appears unaffected by the ZFS.

Following from the above discussion, the two strongest interactions in N@C<sub>60</sub>, the ZFS strain and the hyperfine coupling to the central <sup>14</sup>N nucleus, have little effect on  $T_{2,i}$ . Therefore, some other interactions need to be considered to explain  $T_{2,i}$  and its temperature dependence. Here, we propose that these mechanisms involve nuclear <sup>35</sup>Cl and <sup>37</sup>Cl spins of solvent molecules in the frozen S<sub>2</sub>Cl<sub>2</sub>/CS<sub>2</sub> mixture. The theory of decoherence for electron spins interacting with a bath of nuclear spins (the so-called theory of *spectral diffusion*) has been developed decades ago.<sup>7-9</sup> More recently, the theory has been extended beyond a stochastic treatment

of random nuclear flip-flops to a coherent treatment of all spins together as a single many-body system.<sup>10,28,30</sup> The new theory is also robust to translational diffusion of solvent molecules, covering the fast and slow diffusion regimes, from motional narrowing at high temperatures to the rigid limit at low temperatures. Thus, this theory is ideal for the temperature range studied here. We notice, however, that this theory has been developed for a bath of nuclear spins  $I=1/2$ , and as such it may only be used as an approximation in analyzing our data for  $I=3/2$  of <sup>35</sup>Cl and <sup>37</sup>Cl.

In the rigid limit, i.e., no translational diffusion, the spectral diffusion theory predicts a stretched exponential dependence of the echo decays, e.g.,  $V(\tau)=A \exp[-(2\tau/T_2)^n]$ , with  $2 \leq n \leq 3$ , with  $\tau$  being the delay between pulses in a two-pulse echo experiment.<sup>7-9,28</sup> This dependence seems to be inconsistent with the simple exponential decay,  $V(\tau)=A \exp(-2\tau/T_{2,i})$ , observed in our experiments for N@C<sub>60</sub> in S<sub>2</sub>Cl<sub>2</sub>/CS<sub>2</sub> at all temperatures studied from 20 to 170 K.

An echo decay close to a simple exponential is predicted in the slow diffusion regime, assuming low nuclear spin concentrations.<sup>10</sup> In this case, the echo decay is dominated by a term  $\tau^{9/8}$  in the exponential, which is close enough to be indistinguishable from a simple exponential decay in our experiments. For the CS<sub>2</sub>/S<sub>2</sub>Cl<sub>2</sub> (3/1) mixture used here, we can estimate  $cd^3 < 0.1$  (where  $c$  is concentration of <sup>35</sup>Cl or <sup>37</sup>Cl nuclei and  $d$  is the distance of closest approach between electron and nuclear spins), which satisfies the derived criteria for a low nuclear spin concentration.<sup>10</sup> Using Eq. (3.7) from Ref. 10, we can reproduce the monoexponential decay with  $T_{2,i}=230 \mu\text{s}$  for N@C<sub>60</sub> at 20 K, assuming a diffusion coefficient  $D=5 \times 10^{-16} \text{ cm}^2/\text{s}$  for solvent molecules in CS<sub>2</sub>/S<sub>2</sub>Cl<sub>2</sub>. This  $D$  is small but nevertheless large enough for the exponential term  $\tau^{9/8}$  to dominate over the spin diffusion term  $\tau^2$  expected in the rigid limit.<sup>28</sup>

As temperature increases from 20 K (and, consequently,  $D$  also increases),  $T_2$  is predicted to initially decrease and then increase after reaching a minimum at temperatures where  $D \approx 0.1 \gamma_e \gamma_n \hbar d$ .<sup>28</sup> This minimum corresponds to a transition from the intermediate to fast diffusion regimes; a monoexponential term continues to dominate the spin echo decay in both these regimes. For CS<sub>2</sub>/S<sub>2</sub>Cl<sub>2</sub>, this  $T_2$  minimum is expected to occur at temperatures where  $D = 10^{-10} \text{ cm}^2/\text{s}$ . Comparing with our  $T_{2,i}$  data in Fig. 6, we see that  $T_{2,i}$  indeed develops a minimum at around 100 K. Thus, as temperature increases from 20 to 100 K,  $T_{2,i}$  decreases by 1 order of magnitude (from 230 to 20  $\mu\text{s}$ ) and  $D$  increases by 5 orders of magnitude (from  $10^{-15}$  to  $10^{-10} \text{ cm}^2/\text{s}$ ). This corresponds to an approximate dependence  $T_2 \sim D^{-0.2}$  and thus differs slightly from  $D^{-0.36}$  predicted by the theory for  $I=1/2$ .<sup>28</sup> As temperature increases beyond 100 K,  $T_{2,i}$  increases to 100  $\mu\text{s}$  at 165 K, and we can infer that  $D$  increases only by about an order of magnitude.

To conclude, by comparing our data with the relationship between decoherence rate and diffusion coefficient described in Ref. 28, we infer that  $D$  changes relatively slowly above about 100 K, in contrast to the sharp drop in  $D$  observed below 100 K. This is consistent with the expected behavior around the glass transition temperature  $T_g$ .

## V. CONCLUSIONS

In summary, the effect of nuclear spins in toluene surrounding N@C<sub>60</sub> on the decoherence time has been demonstrated using two different isotopes of hydrogen. The data are fitted well to a model for relaxation by translational diffusion, providing estimates of the diffusion coefficient for C<sub>60</sub> in toluene.

The nuclear spin concentration can be reduced by using a solvent mixture of CS<sub>2</sub> and S<sub>2</sub>Cl<sub>2</sub>. Using such mixture, decoherence times approaching 0.23 ms were observed at temperatures below 20 K, demonstrating this to be a good choice of solvent for low-temperature studies on N@C<sub>60</sub>. Below about 100 K, the outer coherences are not refocused, turning N@C<sub>60</sub> into a “quasi- $S=1/2$ ” spin system. The translational diffusion of local nuclear spins continues to

play a dominant role in decoherence, even for an estimated  $D$  as low as  $10^{-15}$  cm<sup>2</sup>/s.

## ACKNOWLEDGMENTS

We acknowledge helpful discussions with Mark Sambrook and thank the Oxford-Princeton Link fund for support. This research is part of the QIP IRC [www.qipirc.org](http://www.qipirc.org) (GR/S82176/01) and was supported by EPSRC Grant No. EP/D048559/1. J.J.L.M. is supported by St. John’s College, Oxford. A.A. is supported by the Royal Society. G.A.D.B. is supported by the EPSRC (GR/S15808/01). Work at Princeton was supported by the NSF International Office through the Princeton MRSEC Grant No. DMR-0213706 and by the ARO and ARDA under Contract No. DAAD19-02-1-0040.

\*john.morton@materials.ox.ac.uk

- <sup>1</sup>C. Knapp, K.-P. Dinse, B. Pietzak, M. Waiblinger, and A. Weidinger, *Chem. Phys. Lett.* **272**, 433 (1997).
- <sup>2</sup>W. Harneit, *Phys. Rev. A* **65**, 032322 (2002).
- <sup>3</sup>S. C. Benjamin, A. Ardavan, G. A. D. Briggs, D. A. Britz, D. Gunlycke, J. Jefferson, M. A. G. Jones, D. F. Leigh, B. W. Lovett, A. N. Khlobystov, S. Lyon, J. Morton, K. Porfyakis, M. Sambrook, and A. Tyryshkin, *J. Phys.: Condens. Matter* **18**, 5867 (2006).
- <sup>4</sup>E. Dietel, A. Hirsch, B. Pietzak, M. Waiblinger, K. Lips, A. Weidinger, A. Gruss, and K.-P. Dinse, *J. Am. Chem. Soc.* **121**, 2432 (1999).
- <sup>5</sup>J. J. L. Morton, A. M. Tyryshkin, A. Ardavan, K. Porfyakis, S. A. Lyon, and G. A. D. Briggs, *J. Chem. Phys.* **124**, 014508 (2006).
- <sup>6</sup>L. Banci, I. Bertini, and C. Luchinat, *Nuclear and Electron Relaxation* (VCH, Weinheim, 1991).
- <sup>7</sup>J. R. Klauder and P. W. Anderson, *Phys. Rev.* **125**, 912 (1962).
- <sup>8</sup>G. M. Zhidomirov and K. M. Salikhov, *Sov. Phys. JETP* **29**, 1037 (1969).
- <sup>9</sup>A. D. Milov, K. M. Salikhov, and Y. D. Tsvetkov, *Fiz. Tverd. Tela (Leningrad)* **15**, 1187 (1973).
- <sup>10</sup>A. A. Nevzorov and J. H. Freed, *J. Chem. Phys.* **117**, 282 (2002).
- <sup>11</sup>A. D. Bokare and A. Patnaik, *J. Chem. Phys.* **119**, 4529 (2003).
- <sup>12</sup>Q. Ying, J. Marecek, and B. Chu, *J. Chem. Phys.* **101**, 2665 (1994).
- <sup>13</sup>V. N. Bezmel’nitsyn, A. V. Eletsii, and E. V. J. Sepanov, *J. Phys. Chem.* **98**, 6665 (1994).
- <sup>14</sup>S. Nath, H. Pal, D. K. Palit, A. V. Sapre, and J. P. Mittal, *J. Phys. Chem. B* **102**, 10158 (1998).
- <sup>15</sup>R. G. Alargova, S. Deluchi, and K. Tsujii, *J. Am. Chem. Soc.* **123**, 10 (2001).
- <sup>16</sup>L. A. Bulavin, I. I. Adamenko, V. M. Yashchuk, T. Ogul’chansky, Y. I. Prylutskyy, S. S. Durov, and P. Scarff, *J. Mol. Liq.* **93**, 187 (2001).
- <sup>17</sup>S. Nath, H. Pal, and A. V. Sapre, *Chem. Phys. Lett.* **327**, 143 (2000).
- <sup>18</sup>R. S. Ruoff, R. Malhotra, and D. L. Huestis, *Nature (London)* **362**, 140 (1993).
- <sup>19</sup>A. Schweiger and G. Jeschke, *Principles of Pulse Electron Paramagnetic Resonance* (Oxford University Press, Oxford, UK, 2001).
- <sup>20</sup>S. H. Gallagher, R. S. Armstrong, P. A. Lay, and C. A. Reed, *Chem. Phys. Lett.* **248**, 353 (1996).
- <sup>21</sup>S. H. Gallagher, R. S. Armstrong, W. A. Clucas, P. A. Lay, and C. A. Reed, *J. Phys. Chem. A* **101**, 2960 (1997).
- <sup>22</sup>L.-P. Hwang and J. H. Freed, *J. Chem. Phys.* **63**, 4017 (1975).
- <sup>23</sup>J. H. Freed, *J. Chem. Phys.* **68**, 4034 (1978).
- <sup>24</sup>C. F. Polnaszek and R. G. Bryant, *J. Chem. Phys.* **81**, 4038 (1984).
- <sup>25</sup>G. Hinze and H. Sillescu, *J. Chem. Phys.* **104**, 314 (1996).
- <sup>26</sup>M. J. Assael, H. M. T. Avelino, N. K. Dalaouti, J. M. N. A. Fareleira, and K. R. Harris, *Int. J. Thermophys.* **22**, 789 (2001).
- <sup>27</sup>C. A. Angell, B. E. Richards, and V. Velikov, *J. Phys.: Condens. Matter* **11**, A75 (1999).
- <sup>28</sup>A. A. Nevzorov and J. H. Freed, *J. Chem. Phys.* **115**, 2416 (2001).
- <sup>29</sup>R. Perry, D. W. Green, and J. O. Maloney, *Perry’s Chemical Engineer’s Handbook*, 7th ed. (McGraw-Hill, New York, 1997).
- <sup>30</sup>Comparable spectral diffusion theories have been developed more recently, including S. K. Saikin, Wang Yao, and L. J. Sham, *Phys. Rev. B* **75**, 125314 (2007) and W. M. Witzel, R. de Sousa, and S. Das Sarma, *Phys. Rev. B* **72**, 161306 (2005). However, these theories account only for isotropic hyperfine interactions and ignore anisotropic couplings, which make them inapplicable to the N@C<sub>60</sub> case.